

A Regime View of Northern Hemisphere Atmospheric Variability and Change Under Global Warming

A.H. Monahan

Department of Earth and Ocean Sciences, University of British Columbia, Vancouver, BC, Canada

J.C. Fyfe and G.M. Flato

Canadian Centre for Climate Modelling and Analysis, Meteorological Service of Canada, Victoria, BC, Canada

Abstract. The leading mode of wintertime variability in Northern Hemisphere sea level pressure (SLP) is the Arctic Oscillation (AO). It is usually obtained using linear principal component analysis, which produces the optimal, although somewhat restrictive, *linear* approximation to the SLP data. Here we use a recently introduced nonlinear principal component analysis to find the optimal *nonlinear* approximation to SLP data produced by a 1001 year integration of the CCCma coupled general circulation model (CGCM1). This approximation's associated time series is strongly bimodal and partitions the data into two distinct regimes. The first and more persistent regime describes a standing oscillation whose signature in the mid-troposphere is alternating amplification and attenuation of the climatological ridge over Northern Europe, with associated decreasing and increasing daily variance over Northern Eurasia. The second and more episodic regime describes a split-flow south of Greenland with much enhanced daily variance in the Arctic. In a 500 year integration with atmospheric CO₂ stabilized at concentrations projected for year 2100, the occupation statistics of these preferred modes of variability change, such that the episodic split-flow regime occurs less frequently while the standing oscillation regime occurs more frequently.

1. Introduction

Low-frequency variability in atmospheric circulation is usually characterized in terms of space-stationary and time-fluctuating structures such as the North Atlantic Oscillation (NAO), the Pacific-North America pattern (PNA), and the Arctic Oscillation (AO). Of these, the AO has attracted considerable interest recently, both in terms of understanding its observed past behavior [Thompson and Wallace, 1998] and its simulated future behavior under global warming [Fyfe *et al.*, 1999, Shindell *et al.*, 1999]. Recent related investigations [Corti *et al.*, 1999, Smyth *et al.*, 1999] have analyzed the structure of observed hemispheric regimes of atmospheric flow. Here we extend these recent studies by applying a new analysis tool to very long present-day and future-scenario integrations of the CCCma (Canadian Centre for Climate Modelling and Analysis) coupled GCM. We note that the length of the model integrations avoids the limitations imposed by the shortness of the observed hemispheric SLP record.

Copyright 2000 by the American Geophysical Union.

Paper number 1999GL011111.
0094-8276/00/1999GL011111\$05.00

The AO is usually derived using linear principal component analysis (PCA), with the first PC and associated empirical orthogonal function (EOF) together describing the optimal linear approximation to the data. The restriction to linearity of this approximation can have profound implications in that there is no *a priori* reason to believe that the optimal approximation to a general data set is linear. Given data $\mathbf{X}(t)$ in M spatial dimensions at N times we remove this restriction by considering a pair of (generally nonlinear) functions s_f and \mathbf{f} where s_f maps $\mathbf{X}(t)$ onto a single time series and \mathbf{f} maps that time series back onto an approximation $\hat{\mathbf{X}}(t)$ in the space of the M spatial dimensions. s_f and \mathbf{f} are determined such that $\hat{\mathbf{X}}(t)$ is the optimal approximation to $\mathbf{X}(t)$ in the least squares sense. If the functions are constrained to be linear this is simply PCA with the time series associated with s_f being the linear PC and The spatial map associated with the function \mathbf{f} being the linear EOF. If the functions are not constrained to be linear we have the present nonlinear PCA (or NLPCA). This method and the exact procedure for obtaining these functions is detailed in Monahan (1999).

In this paper, we apply NLPCA to Northern Hemisphere (north of 20°N) wintertime (November–April) monthly-mean SLP produced by the CCCma coupled climate model. To make the analysis tractable, this data is first projected onto the space of its 10 leading linear EOFs (so $M = 10$). We investigate the NLPCA characterization of large-scale variability in Northern Hemisphere circulation, and additionally, investigate changes in the diagnosed patterns and temporal characteristics under global warming. The coupled model is described in Flato *et al.* (1999). It is a global primitive equation spectral model with T32 triangular truncation and 10 unequally-spaced vertical levels with the top level at 12 hPa. The ocean component is a global primitive equation grid-point model with 1.875° resolution and 29 vertical levels. This model displays realistic AO variability, as described by Fyfe *et al.* (1999). The data considered here are from a 1001 year control integration and a 500 year stabilization integration in which greenhouse gases and aerosol forcing are fixed at their year 2100 levels following a transient simulation from 1850 to 2100.

2. Control Integration

Figure 1 displays the results of the NLPCA of SLP data from the control integration. This NLPCA approximation explains 27% of the total variance in SLP, in contrast to the leading linear PC which explains 24% of the total variance. The time series $\alpha(t) = s_f(\mathbf{X}(t))$ describes the temporal vari-

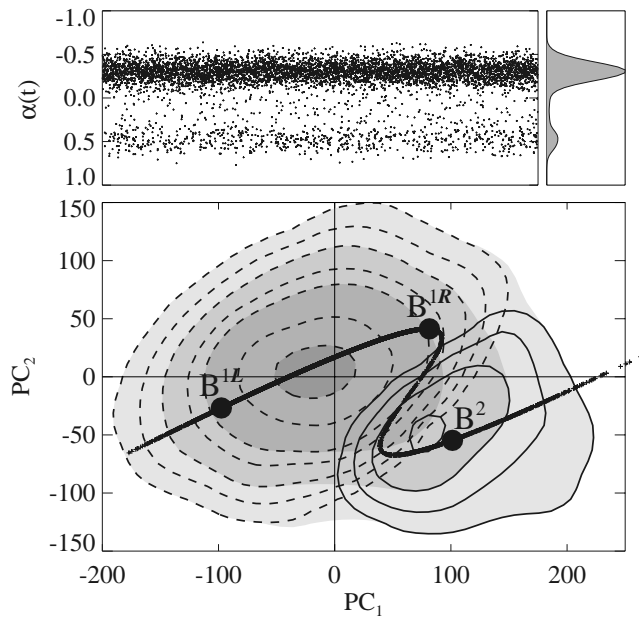


Figure 1. NLPCA from a 1001-year control simulation. Top-left: $\alpha(t)$. Top-right: $\alpha(t)$ PDF. Bottom: Z-shaped curve is $\hat{\mathbf{X}}(t)$ in the space of the two leading linear PCs. Total (shaded), Branch 1 (dashed) and Branch 2 (solid) PDFs have contour values of 2, 5, 10, 20, 30, 60 and 90 percent of the total maximum.

ability of the NLPCA approximation, and is displayed in the upper left panel of Figure 1, along with its probability density function (PDF) in the upper right panel. Importantly, the PDF is characterized by two distinct peaks, demonstrating the existence of two well-separated regimes. Inspection of $\alpha(t)$ indicates that the NLPCA approximation describes oscillatory behavior within the populous upper band of points with episodic excursions to the lower band where the system remains for no longer than a month or two at a time.

The spatial characteristics of the NLPCA approximation are obtained from the Z-shaped curve in the bottom panel of Figure 1. A given point on the Z-shaped curve represents the NLPCA approximation $\hat{\mathbf{X}}(t)$ at a given time in the space spanned by the two leading linear PCs (PC_1 and PC_2). In general, such a curve would project into the space of the other linear PCs however in this particular case those projections are negligible. As such, the spatial map corresponding to the approximation at a given time is simply obtained by reading off the values of PC_1 and PC_2 at the point on the Z-shaped curve and then weighting and adding the corresponding linear EOFs (EOF₁ and EOF₂). For reference, EOF₁ and EOF₂ are shown in Figure 1 of *Fyfe et al.* (1999), with the former representing the model rendition of the observed AO.

We note that the upper segment of the Z-shaped curve (hereafter Branch 1) in Figure 1 is associated with the populous upper band of points in $\alpha(t)$, while the lower segment of the curve (hereafter Branch 2) corresponds to the much less populous lower band of points in $\alpha(t)$. The marginal PDF of the two leading linear PCs is shaded in the bottom panel of Figure 1. It is markedly (and statistically) non-Gaussian in shape, displaying in particular a pronounced lobe in the lower right. Also illustrated is the marginal PDF using only those PC_1 and PC_2 points that map onto Branch

1 (dashed contours) and the marginal PDF using only those PC_1 and PC_2 points that map onto Branch 2 (solid contours). The Branch 1 distribution is very nearly Gaussian and is well-characterized by the NLPCA approximation, which describes its primary axis of variability. Branch 2 also runs through the middle of its PDF.

The NLPCA approximation differs from the PCA approximation in that, while it is associated with a single time series, it is not associated with a single spatial pattern. As time evolves, $\hat{\mathbf{X}}(t)$ describes a sequence of spatial patterns. Figure 2 displays SLP maps derived as composites over points in the neighborhoods of three representative points on $\hat{\mathbf{X}}(t)$: points B^{1L} and B^{1R} are associated with Branch 1, and point B^2 with Branch 2. The B^{1L} composite is characterized by anomalies of opposite sign over the polar regions and the mid-latitudes, with a strong negative SLP anomaly over northwestern Russia and weaker positive extrema over the region of the Aleutian Low and over the western Mediterranean. The B^{1R} composite differs from the B^{1L} composite primarily in sign. Thus, variability along Branch 1 of $\hat{\mathbf{X}}(t)$ essentially describes a standing oscillation, the positive and negative phases of which are respectively illustrated by the B^{1L} and B^{1R} composites. We note that the Branch 1 oscillation resembles the AO (i.e. EOF₁) but with its high latitude centre of action shifted eastward relative to the AO, by virtue of a contribution from EOF₂.

The B^2 composite is similar to the B^{1R} composite in that it is characterized by oppositely-signed SLP anomalies over the polar regions and mid-latitudes. However, the high latitude extremum has shifted about 90° westward to a point near Iceland, and mid-latitude anomalies are dominated by a centre near the Azores. This pattern strongly resembles a large amplitude negative phase of the NAO. Note that unlike Branch 1, in which the patterns appear in both positive and negative phases, on Branch 2 the patterns occur only with a single sign. It is important to note that it is not suggested here that the NAO is realized in the model in only one phase and only rarely. Indeed, the model NAO index (defined traditionally as the difference in SLP between Iceland and the Azores) does regularly visit both positive and negative values. What is being stated here is that a pattern resembling the extreme negative phase of the NAO appears as a distinct, albeit episodic, regime in a hemispheric SLP NLPCA.

Figure 3 (top) displays maps of composite 500 hPa geopotential height (Z_{500}) associated with the three points described previously. B^{1L} and B^{1R} describe attenuation and amplification of the climatological ridge over Europe, respec-

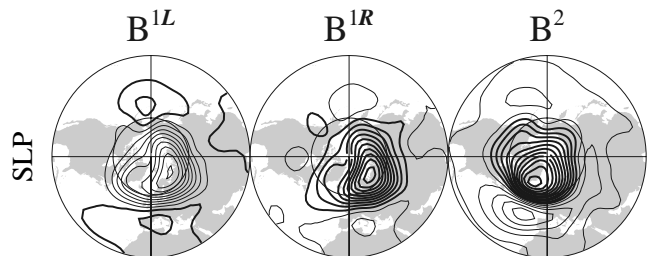


Figure 2. SLP anomaly maps derived as composites over neighborhoods of the three representative points on $\hat{\mathbf{X}}(t)$ of Figure 1. Contours for SLP are 1 hPa (...-1.5,-0.5,0.5...). Thick contours are positive and thin contours are negative.

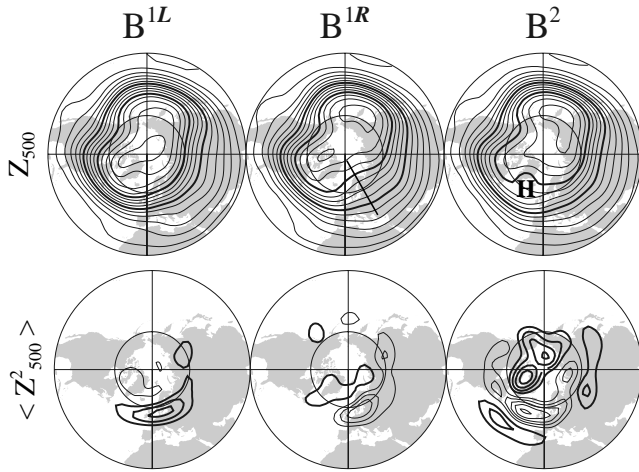


Figure 3. Top: Monthly-mean Z_{500} composites with contours in DM (500, 505, ...). Bottom: Intra-monthly daily variance $< Z_{500}^2 >$ composites with contours in DM² (50, 100,...).

tively. As seen in Figure 3 (bottom) this is associated with changes in intra-monthly daily variance $< Z_{500}^2 >$. Specifically, when the European ridge is amplified there is a decrease in daily variance over Northern Eurasia, and vice versa. The Z_{500} B^2 composite displays a strengthened western North America ridge and a flow which is split around a local anti-cyclone south of Greenland. Downstream of both regions there is decreased daily variance while north of both regions there is greatly enhanced daily variance (presumably as synoptic storms are steered northward, but also possibly involving enhanced baroclinicity). We note that the Branch 2 spatially-averaged anomalous daily variance in the Arctic (north of 60°N) is ten times that found anywhere on Branch 1.

We conclude this subsection by noting that all the results reported here, and to follow, are completely robust in terms of being unchanged when subsets of the data sets are used.

3. Behavior in a Warmer Climate

Here projection time series were obtained by projecting the ten leading control linear EOFs onto the SLP data from the 500-year stabilization run. Figure 4 displays the time series $\alpha(t)$ (top) and the NLPCA approximation $\hat{\mathbf{X}}(t)$ in the space of the two leading control integration PCs (bottom). Under global warming, bimodality in $\alpha(t)$ vanishes and $\hat{\mathbf{X}}(t)$ extends out into the upper right (i.e., without branching, as in the control integration). Consideration of the associated spatial patterns reveals that under global warming, Branch 1 variability does not significantly alter, but that it becomes a more frequented mode of climate variability, at the expense of less frequented North Atlantic split-flow events. Note that the approximation $\hat{\mathbf{X}}(t)$ is tilted (rather than horizontal as might be expected) relative to the PC_1 axis in Figure 4 because the PC_1 and PC_2 axes are those obtained from the control integration. These results are broadly consistent with the suggestion by Palmer (1999) that the climate response to external forcing (in this case, roughly quadrupled atmospheric CO₂) is a change in the occupation statistics of the preferred modes of variability, rather than changes in the modes themselves.

4. Summary and Discussion

A nonlinear principal component analysis of Northern Hemisphere variability in a CCCma coupled model control integration shows the main zonal asymmetry being in either of two distinct states: one being very frequented and involving fluctuations in the amplitude of the climatological ridge over western Europe, and the other being rarely visited and involving a split-flow configuration south of Greenland. The linear PCA view used previously (of either observed or simulated variability) sees the main zonal asymmetry as residing in the North Atlantic and involving fluctuations in the amplitude of the Icelandic Low and Azores High (i.e., being the NAO-related component of the AO). Indeed, it has been suggested that the AO be renamed the “Arctic-Atlantic Oscillation” [Deser, A note on the Annularity of the “Arctic Oscillation”, submitted to *Geophys. Res. Lett.*, 1999]. However, based on our nonlinear analysis we conclude that, by virtue of the non-Gaussian nature of model SLP, Northern Hemisphere variability is better characterized as an “Arctic-Eurasia Oscillation” which occasionally, but significantly, is replaced by a split-flow configuration in the North Atlantic (the linear view apparently being a compromise between these two distinct states).

As to the relevance of our model-based results to the real world we quote from the observational study of Nakamura and Wallace (1991): “Large skewness at a particular location might be indicative of a juxtaposition of two flow regimes: one which prevails most of the time and another which occurs relatively infrequently and is therefore characterized by large anomalies”. [Significant skewness, or normalized third statistical moment, being indicative of non-Gaussian distributions.] The model Northern Hemisphere SLP skewness (not shown) is most strongly positive over Greenland, which in the model is the region of infrequent but anomalously large North Atlantic split-flows. Interestingly,

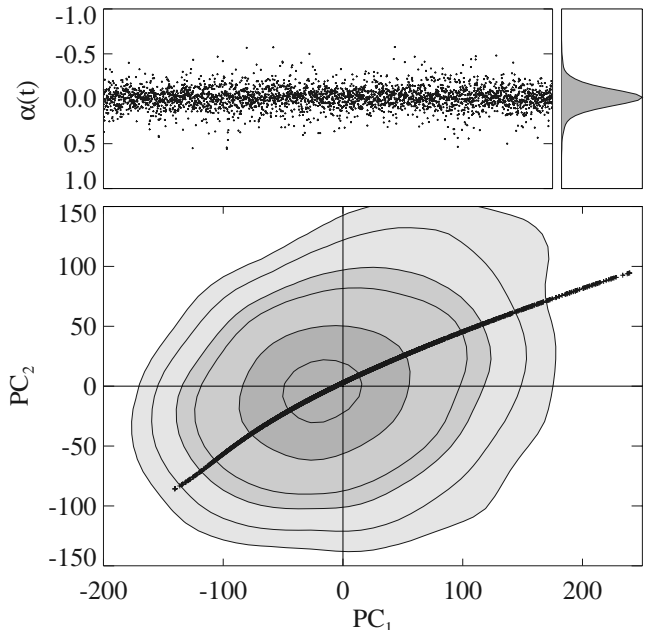


Figure 4. As in Figure 1 but for a 500 year integration with CO₂ and aerosolforcing stabilized at levels projected for the year 2100.

the observed SLP skewness [Nakamura and Wallace, 1991] is also strongly positive over this region, suggesting that our model-based view of Northern Hemisphere variability may well carry over to the real world.

Acknowledgments. We are grateful to J. Scinocca and S. Kharin for comments on an earlier draft of this paper, and to S. Tinis for assisting in the data manipulation.

References

- Corti, S., F. Molteni, and T.N. Palmer, Signature of recent climate change in frequencies of natural atmospheric regimes, *Nature*, 398, 799-802, 1999.
- Flato, G.M., G.J. Boer, W.G. Lee, N.A. McFarlane, D. Ramsden, M.C. Reader and A.J. Weaver, The Canadian Centre for Climate Modelling and Analysis Global Coupled Model and its Climate, *Climate Dynamics*, in press 1999.
- Fyfe, J.C., G.J. Boer, and G.M. Flato, The Arctic and Antarctic oscillations and their projected changes under global warming, *Geophys. Res. Lett.*, 26, 1601-1604, 1999.
- Monahan, A.H., Nonlinear principal component analysis by neural networks: theory and application to the Lorenz system, *J. of Clim.*, 13, 821-835, 2000.
- Nakamura, H. and J.M. Wallace, Skewness of low-frequency fluctuations in the tropospheric circulation during the northern hemisphere winter, *J. of Atmos. Sci.*, 48, 1441-1448, 1991.
- Palmer, T.N., A nonlinear dynamical perspective on climate prediction, *J. of Clim.*, 12, 575-591, 1999.
- Shindell, D.T., R.L. Miller, G.A. Schmidt, and L. Pandolfo, Simulation of recent northern hemisphere climate trends by greenhouse-gas forcing, *Nature*, 399, 452-455, 1999.
- Smyth, P., K. Ide, and M. Ghil, Multiple regimes in northern hemisphere height fields via mixture model clustering, *J. Atmos. Sci.*, 56, 3704-3723, 1999.
- Thompson, D.W. and J.M. Wallace, The Arctic Oscillation signature in the wintertime geopotential height and temperature fields, *Geophys. Res. Lett.*, 25, 1297-1300, 1998.

A.H. Monahan, Department of Earth and Ocean Sciences, University of British Columbia, Vancouver, BC, Canada (email: monahan@ocgy.ubc.ca)

G.M. Flato and J.C. Fyfe, Canadian Centre for Climate Modelling and Analysis, Meteorological Service of Canada, University of Victoria, PO Box 1700, Victoria, BC, Canada V8W 2Y2. (email: Greg.Flato@ec.gc.ca, John.Fyfe@ec.gc.ca)

(Received September 28, 1999; revised December 14, 1999; accepted February 14, 2000.)